Advances in Science and Technology Research Journal

Advances in Science and Technology Research Journal, 2027, 21(1), 65–85
https://doi.org/10.12913/22998624/231209
ISSN 2299-8624, License CC-BY 4.0

Received: 2026.07.26
Accepted: 2026.11.15
Published: 2026.12.01

Effect of a support insert on the post-machining deformation in a thin wall milled at a maximized axial depth of cut

Magdalena Zawada-Michałowska[1*], Paweł Pieśko[1]

[1] Lublin University of Technology, Faculty of Mechanical Engineering, Department of Production Engineering, Nadbystrzycka 38D, 20-618 Lublin, Poland
* Corresponding author's e-mail: m.michalowska@pollub.pl

ABSTRACT

The aim of the present research was to evaluate the effect of a support insert made of a silicone casting resin on reducing the post-machining deformation in thin walls made of 7050 T7451 aluminum alloy during finish milling at a maximized axial depth of cut. Experiments were conducted on the samples with 48 mm high walls and three different thicknesses (t = 1–2 mm, with the step of 0.5 mm), using three cutting speeds (v_c = 300–900 m/min, with the step of 300 m/min). Statistical reliability of the obtained results was achieved through the application of a face-centered central composite design (FCCCD) and Response Surface Methodology (RSM). Post-machining deformation was evaluated based on flatness and wall thickness deviations that were measured via active scanning with a Zeiss Contura coordinate measuring machine. The results showed that an increase in the wall thickness reduced the post-machining deformation, while the impact of the cutting speed was nonlinear. The highest values of both flatness and wall thickness deviations were obtained using the mid-range cutting speeds, whereas significantly better results were produced at the extreme speeds (v_c = 300 m/min and v_c = 900 m/min). An examination of the surfaces in the thin-walled samples with a simple geometry revealed no characteristic signs of chatter. This finding is particularly important, as the tested parts had an open structure, which is exceptionally prone to chatter. The experimental findings indicate the effectiveness of using a support insert in thin-wall milling at a maximized depth of cut, demonstrating the solution's potential in high-performance machining for aerospace components.

Keywords: thin-walled element, post-machining deformation, strain, milling, aluminum alloy, RSM, support insert.

INTRODUCTION

In modern industry, milling is one of the most frequently used processes for producing engineering parts, especially those requiring high precision. A significant challenge is the machining of integral thin-walled structures, particularly since these are often large-sized components [1]. A key rationale behind using such elements is their weight, which affects not only flight performance but also operating costs [2]. Aluminum alloys are widely used materials for their production [3]. Typical aerospace applications of thin-walled parts include components for wings, tails, and fuselages [4]. In many cases, they are characterized by a uniform structure, which is why they are normally manufactured from monolithic rolled plates, where more than 90% of the mass is converted into chips during machining. Despite their advantages, thin-walled parts exhibit relatively low stiffness, increasing their susceptibility to machining deformation [5]. Wang et al. [6], citing Boeing reports, indicated that the probability of deformation in thin-walled aerospace elements, leading to the exceeding of specified tolerances, is nearly 50%, while the estimated costs associated with production defects or the need for additional corrections amount to hundreds of millions of dollars annually. The post-machining deformation of these structures is the main cause of parts being scrapped, which is one of the greatest problems in the aerospace industry [7]. It should also be

noted that this applies to industries such as the automotive, shipbuilding, and military sectors. It results from the fact that components with thin walls are widely used in the production of automobiles, ships, and military equipment [8,9]. For this reason, many researchers around the world, often in collaboration with industrial partners, are conducting research into ways of minimizing this deformation in thin-walled structures and gaining a thorough insight into the mechanisms behind its formation [10]. Nevertheless, the problem of post-machining deformation remains highly complex, as the quality of the manufactured part results from the coupled interaction between material, geometric, technological, and dynamic factors [11].

The post-machining deformation of thin-walled components primarily results from the redistribution of residual stresses [12], which can be released both during the production of a semi-finished product (e.g., by rolling, casting, heat treatment) and during machining [13,14]. The removal of a layer of material disrupts the equilibrium of stresses, which, in the case of structures with low stiffness, results in their distortion [15,16]. Another significant factor affecting the accuracy of machined parts is self-excited vibration (chatter) [17,18]. Its occurrence leads to machining instability by generating a variable cutting force, resulting in considerable part distortion [19]. The impact of chatter on thin-walled parts is extremely significant, as even small vibration amplitudes can significantly reduce the accuracy of manufactured elements [20]. With such components, the gradual removal of material modifies their mechanical and dynamic properties. The decrease in the stiffness and the resulting shifts in natural frequencies, along with changes in vibration modes, cause the dynamic characteristics of the machining system to undergo continuous modification during milling [21]. Therefore, one key factor determining the process stability and the surface quality of machined thin-walled parts is the dynamic rigidity of the entire machine tool-holder-workpiece-tool system, as it affects the system's susceptibility to chatter and, consequently, to post-machining deformation in these structures [22,23].

In the literature of the subject, the emphasis is placed on the dependence of post-machining deformation on many factors, including the material's mechanical properties and manufacturing history, as well as workpiece geometry [24]. The sequence of machining operations [25], tool selection [26], cutting parameters [27], and clamping method [28] are also of fundamental importance. Even minor changes in the configuration of the manufacturing process for thin-walled components can lead to significant differences in their final dimensional and geometric accuracy. An important research problem is therefore to develop technological solutions that would minimize the formation of such distortions. Considering these challenges, various solutions for process control are analyzed, including, among others, tool path optimization [29], symmetric allowance removal [30], and the use of deformation compensation techniques [31]. In addition, a key area of research, which enables the prediction and monitoring of distortion occurrence, is the use of numerical methods or artificial intelligence [32,33].

A significant number of researchers have also focused on developing concepts for clamping thin-walled parts to minimize chatter during machining. This focus stems from the fact that the clamping system plays a crucial role under such machining conditions, and proper support as well as workpiece stabilization can substantially increase dynamic stiffness and process stability. Liang et al. [34] presented an innovative clamping solution, referred to as a flexible fixture system, designed for milling thin-walled components that are susceptible to chatter. This solution was based on conformal, flexible clamping elements that adapted to the part's geometry, ensuring a uniform force distribution and increased contact area. This provided additional damping at the workpiece-fixture interface, which improved the dynamic properties of the entire machining system. Additionally, they developed a dynamic model describing the impact of clamping conditions on the process stability limits, demonstrating that the stable operating range could be extended. The experimental findings confirmed a significant reduction in vibration amplitude. Liu et al. [35] evaluated the influence of air jet assistance on the stability of milling a thin-walled Ti6Al4V titanium alloy part. Experiments were performed to compare the effects of machining conducted with and without additional air-jet assistance using identical milling parameters, with particular emphasis on cutting force and vibration acceleration signals. A frequency-domain signal analysis showed that the force generated by the air jet significantly contributed to the stabilization of the thin-walled part, leading to reduced vibration and decreased cutting force. The authors concluded

that the additional dynamic load induced by the air jet improved the system's stiffness and the tool-workpiece contact conditions, thereby contributing to improved machining quality. Fei et al. [36] proposed a novel concept of a movable fixture that was designed to reduce the milling-induced deformation of thin-walled components. This developed method used a single support located on the side of the wall opposite the cutting zone, which was moving along with the tool at the same speed. This provided local stiffening of the material precisely at the point of cutting force application. The study also introduced a dynamic model describing the tool-workpiece-movable support interaction. The experimental results confirmed that the solution significantly reduced both distortion in thin-walled parts and vibration amplitude. Wan et al. [37] also investigated an approach to chatter suppression during the milling of thin-walled components, using a fixture that moved along with the tool to provide a local increase in stiffness and reduce vibration directly in the cutting zone. This solution led to mitigating chatter throughout the entire process without the need for using additional damping systems. The study developed a dynamic model of the milling process that accounted for changes in the workpiece dynamic properties caused by material removal and contact with the moving fixture. Based on this model, stability lobe diagrams were determined for this concept. The numerical and experimental results confirmed that the moving fixture effectively increased the stable machining range and reduced chatter occurrence during the milling of thin-walled elements. A method for chatter suppression during machining of such parts via controllable magnetic-field-induced magnetorheological fluid solidification was developed by Liu et al. [38]. The proposed method involved filling the space around the workpiece with this special fluid, the properties of which changed following the application of a magnetic field. Under such conditions, ferromagnetic particles in the fluid formed chain-like structures, causing the material's transition into a quasi-solid state and increasing its stiffness. This made it possible to achieve adaptive vibration suppression in the machining zone. The authors demonstrated that the magnetic field strength control could effectively shift the process stability limits and reduce the chatter occurrence when machining parts with thin walls.

A particularly interesting direction for future research appears to be the application of Minimum Quantity Lubrication (MQL) in the machining of thin-walled components, especially those made of difficult-to-machine materials. In the case of titanium alloys, dry machining is often associated with substantial costs resulting from intensive tool wear [39,40]. Therefore, the implementation of MQL may offer a promising approach for improving both process sustainability and economic efficiency while maintaining the required machining quality. In addition, its use may also contribute to the reduction of vibrations and improve the dynamic stability of the cutting process [41].

Growing demand for enhanced manufacturing efficiency stimulates an increasing interest in milling strategies that would enable more intensive material removal. One such strategy is milling at the maximized axial depth of cut, also referred to as full wall height milling [42,43]. It is an alternative to conventional machining methods, which involve performing a sequence of multiple tool passes alternately on either side of the wall [44,45]. Unlike conventional methods, this type of milling is performed with small values of the radial depth of cut while engaging nearly the entire working length of the tool. However, these conditions markedly alter the nature of interactions that occur in the cutting zone. The load is distributed across the entire height of the wall being machined, which increases its susceptibility to deflection and dynamic phenomena associated with a loss of process stability [46]. Additionally, the need to use end mills with a significant overhang, particularly when milling high walls, promotes deflection of both the tool and the workpiece due to the action of the cutting force [47,48]. Under such conditions, the manufacturing accuracy of the part depends not only on the process parameters and tool geometry, but also on the dynamic workpiece-cutter interaction. For this reason, new solutions for clamping and supporting thin-walled elements are of particular importance, as their purpose is to reduce local distortions, improve vibration damping, and increase the system's resistance to dynamic instabilities [49,50]. Consequently, the stability of the milling process depends not only on the properties of the spindle and the tool, but also on the dynamic behavior of the entire machine tool-holder-workpiece-tool system and its ability to resist the forces generated during machining [51].

Summing up, despite numerous studies devoted to reducing post-machining deformation in thin-walled parts, many of the approaches

proposed to date rely on advanced clamping systems, active and passive vibration-damping systems, or specialized supports that move along with the cutting zone. However, these solutions are characterized by high structural complexity, high implementation costs, and the need for additional control systems and integration with the machine tool, which limits their use in industrial settings. Consequently, it is necessary that less complex and more cost-efficient methods be developed for improving thin-walled component machining conditions.

The primary goal of this study was to evaluate the potential for reducing post-machining deformation in thin walls by using a support insert made of a silicone casting resin during finish milling at a maximized axial depth of cut. The developed solution serves as an alternative to currently used specialized support systems, as it does not require modifications to the machine tool or additional systems, and can be easily adapted to the geometry of the workpiece. Particular emphasis was placed on assessing the effectiveness of using the insert under variable wall thickness at different cutting speeds. The developed approach was analyzed based on changes in flatness and wall thickness deviations, both serving as measures of post-machining deformation in thin walls.

METHODOLOGY

First of all, an experimental plan was designed, and factors that could affect both the stability of the analyzed process and the research results were identified. A thin-walled sample with a simple geometry was chosen as the main focus of the study, and experimental variables were defined. Independent variables included the wall thickness of a test sample and the cutting speed used in finish milling at a maximized axial depth of cut. The post-machining deformation of a thin wall was quantified using two dependent variables: flatness deviation and wall-thickness deviation. To enable a reliable comparison of the results, a set of parameters was also defined that were maintained constant throughout the experiment. This group included feed per tooth, axial depth of cut, radial depth of cut, and end mills.

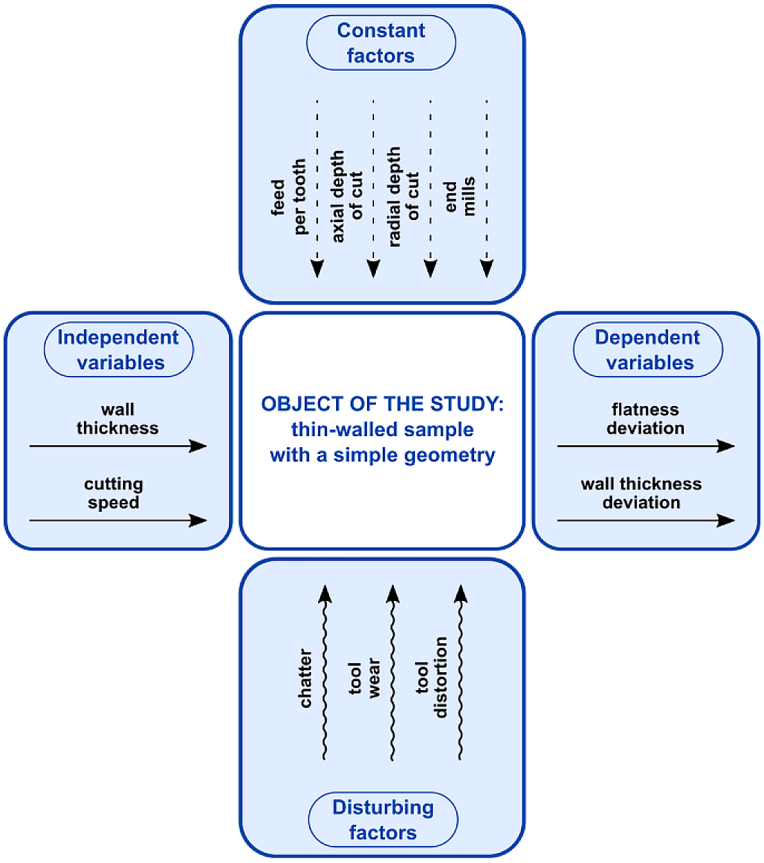


Figure 1. Experimental plan

The experiment planning phase also included the consideration of potential disturbing factors that could influence the accuracy and repeatability of the results. Particular emphasis was placed on the possibility of chatter, tool wear, and tool deflection during machining. The plan designed in this way served as the basis for carrying out the subsequent stages of the experiment (Figure 1).

To ensure statistically reliable results of the research on thin-wall milling using a support insert, the Design of Experiments (DoE) method was employed. This approach enabled a rational selection of the number of test runs and the development of mathematical models describing the relationships between independent and dependent variables. Additionally, the use of DoE allowed for the optimization of machining conditions within the analyzed parameter range, with the criterion being the minimization of post-machining deformation in the tested thin-walled element. Design-Expert® (version: 23.1.8) was used to develop an experimental design and perform a statistical analysis of the results. Experiments were planned according to response surface methodology (RSM) using a face-centered central composite design (FCCCD). This design included two quantitative input variables: wall thickness (A) and cutting speed (B). Each of the analyzed variables was considered at three levels, as shown in Table 1. This concept made it possible to determine not only the linear effects of individual parameters but also the quadratic effects and interactions between the tested variables. The optimized experimental matrix comprised thirteen test runs, including five replicates of the central point, aimed at evaluating experimental variability and assessing the repeatability of the results. The remaining combinations were tested as single experimental runs (according to the FCCCD principle). This adopted experimental design provided sufficient data to construct regression models and conduct a statistical significance analysis of the influence of individual factors on the process responses under study.

After developing the experimental design, the experimental stage began with the fabrication of an insert for supporting the thin wall during finish milling. The main purpose of this insert was to reduce chatter marks by improving the support conditions for the wall and increasing the stiffness of the workpiece-cutter system. The insert was manufactured by the gravity method, using BLUESIL RTV 3318 silicone elastomer with the following properties [52]: tensile strength $S_b = 3.3$ MPa, elongation at break $\varepsilon_b = 520\%$ (designations in accordance with ISO 37:2024 [53]), and tear strength $TR = 19$ kN/m (designation in accordance with ISO 34-1:2024 [54]). The process of preparing the insert began with the fabrication of a mold made of aluminum alloy. To facilitate the mold release, the inner surfaces of the mold were coated with the release agent Buehler 20-8185-002. Next, the mixture was prepared by mechanically mixing BLUESIL RTV 3318 resin with BLUESIL CATA 6H catalyst in a 20:1 weight ratio. The resulting mixture was poured into the mold, ensuring that the mold was filled evenly and that the top surface of the molded piece was leveled. According to the manufacturer, the recommended curing time of 6 hours corresponds to the minimum time required to achieve initial strength under standard ambient conditions. In the present study, the support insert was left to cure for approximately 24 hours in order to ensure more complete cross-linking of the material and stabilization of its mechanical properties, thereby improving the repeatability and reliability of the experimental results. Once this process was complete, the finished insert was removed from the mold and used in subsequent stages of the experiment. To ensure proper contact conditions at the insert-thin wall interface and to increase the support performance, an additional clamp was fixed opposite the surface being machined. It should be noted that contact repeatability and the support insert application conditions in the adopted experimental configuration were ensured by maintaining the same assembly procedure for all experimental runs. Furthermore, proper clamping was achieved by appropriately selecting the thicknesses of the support insert and the additional clamp. The test sample with a support insert is shown in Figure 2.

Thin-walled samples with a simple geometry were machined from 7050 aluminum alloy

Table 1. Experimental design – FCCCD

Independent variable	Symbol	Unit	Code	Low level (-1)	Medium level (0)	High level (+1)
Wall thickness	t	mm	A	1	1.5	2
Cutting speed	v_c	m/min	B	300	600	900

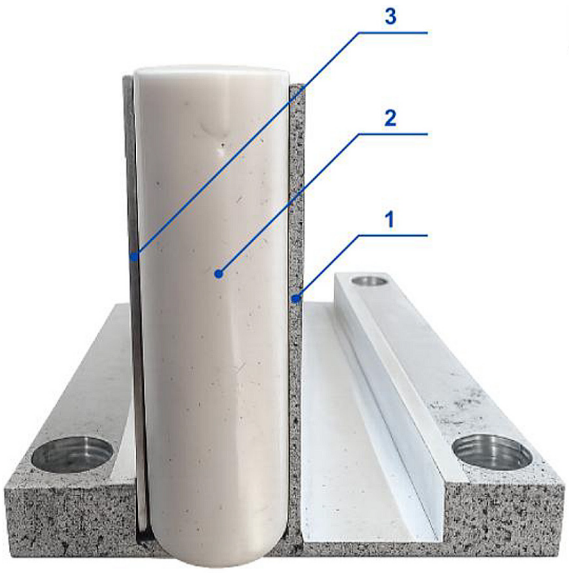


Figure 2. Thin-walled sample with a support insert: 1 – thin wall, 2 – support insert, 3 – clamp

(state: T7451). This material was selected owing to its high strength and relatively low density, as well as its widespread use in thin-walled structures exposed to high operational loads. It should be noted that its specifications comply with the AMS4050K standard [55]. A 50 mm-thick rolled plate was used as the semi-finished product, from which rectangular blocks 100 mm long and 65 mm wide were cut out. Machining was performed on an Avia VMC 800HS machine tool. First, the samples were clamped in a machine vise for preliminary machining, which involved removing excess material and fabricating mounting holes for the subsequent operation. After that, the workpiece was bolted to a specially prepared mounting plate. This solution ensured the repeatability of workpiece clamping in the holder and eliminated its impact on the part's accuracy. In the next phase, the actual machining was performed, consisting of the complete milling process, i.e., roughing and finishing. The technological parameters of roughing were maintained at a constant level corresponding to high-performance cutting (HPC), wherein the radial depth of cut a_e was determined based on the wall thickness and selected such that its value at the wall was constant a_e = 10.4 mm. The finishing operation was carried out at the maximum depth of cut, in two passes – starting from the left side of the wall and then proceeding to the right side. It should be added that a support insert was used to support the thin wall. It was positioned on the non-machined side of the wall (Figure 3). This operation was performed by the dry down-milling method. KYOCERA SGS end mills were used for the actual machining; specifically, tool 44985 (d = 16 mm, L = 108 mm, z = 3) was used for roughing, and tool 44748 (d = 12 mm, L = 100 mm, z = 4) for finishing. For both cases, ERICKSON AHPVTTMQL1C heat-shrink tool holders were used to secure the tools (rough milling: 16090M, finish milling: 12090M). After each experimental run, the cutting tool was visually inspected to monitor its condition. Following the completion of all machining tests, an additional assessment was performed using an optical microscope. The observations did not indicate any substantial wear or damage that might have affected the experimental results or the evaluated response parameters. As a result, thin-walled samples with a simple geometry were produced, the walls of which had a height of h = 48 mm and varying thicknesses of t = 1 mm, 1.5 mm, or 2 mm, respectively (another tested independent variable). Table 2 presents a summary of

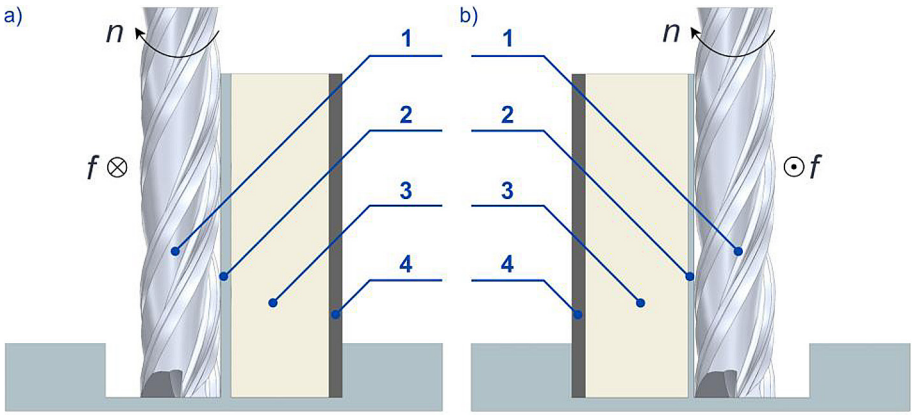


Figure 3. Finish milling of a thin-walled element: a) first tool pass – left side, b) second tool pass – right side: 1 – end mill, 2 – machined thin wall, 3 – support insert, 4 – clamp

Table 2. Summary of technological parameters used during the actual machining of the thin wall

Technological parameters	Roughing operation	Finishing operation
Cutting speed v_c [m/min]	900	300, 600, and 900
Feed per tooth f_z [mm/tooth]	0.05	0.025
Axial depth of cut a_p [mm]	5 and 3 (for the final tool pass)	48
Radial depth of cut a_e [mm]	8.9 (t = 1 mm) or 8.65 (t = 1.5 mm) or 8.4 (t = 2 mm) and 10.4 (constant for all t)	0.2

the machining parameters used during the actual thin-wall machining process, while Figure 4 shows successive stages of the machining process for a thin-walled component with simple geometry (Figure 4a), along with a view of the finished part (Figure 4b).

The evaluation of post-machining deformation was a key part of this study. To quantitatively determine changes in the thin wall geometry after milling with a support insert, flatness deviation (f_d) and wall thickness deviation (t_d) were used as response variables. They were measured using a Zeiss Contura coordinate measuring machine in a configuration of 7/10/6 operating with a VAST XT GOLD scanning head. Calypso 2023 software supported the measurement procedure and data processing. The active scanning technique was employed. Furthermore, owing to the high sampling density, the flatness deviation allowed not only for a quantitative assessment of the degree of wall deformation but also for a qualitative analysis in 3D form. All samples were measured following the same procedure using a datum reference frame. Both measures of post-machining deformation (i.e., flatness and wall thickness deviations) were measured using a strategy known as Raster, which consists of systematic parallel scanning paths distributed uniformly over the measured surface in a grid-like pattern. However, for flatness deviation measurement, the probe moved horizontally, i.e., parallel to the longer edge of the sample (Figure 5a), while for wall thickness deviation measurement, it moved vertically, i.e., perpendicular to the longer edge of the sample (Figure 5b). The flatness deviation was examined for the same functional surface in each sample. The wall thickness was determined between two surfaces at their upper part with a 3 mm offset from the wall edge. The wall thickness deviation was calculated as the difference between the thickness measured at the upper part of the wall (3 mm from the top edge) and the nominal thickness. This approach was adopted because the machined walls exhibited a characteristic trapezoidal shape. The scanning step was 0.1 mm, the scanning speed was 10 mm/s, and approximately 19,000 measurement points were acquired. During data processing, a Gaussian low-pass filter was applied, together with an outlier removal procedure based on five neighboring points (standard CMM evaluation).

Consequently, reducing these deviations was equivalent to limiting the deformation of the tested wall after machining, which, in the adopted approach, served as the basis for evaluating the reduction in post-machining deformation. The

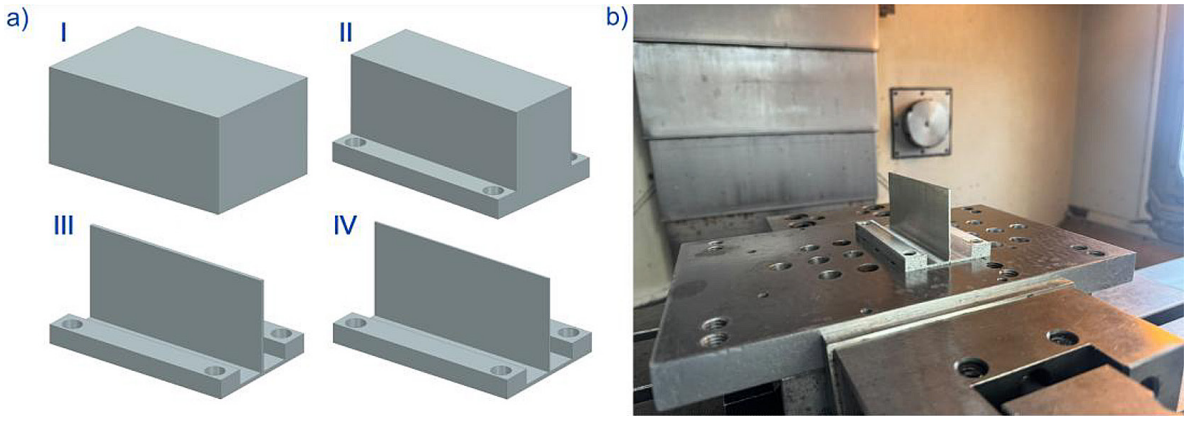


Figure 4. Machining of a thin-walled element with a simple geometry: a) stages of machining, b) view of a finished part: I – rectangular block, II – sample after pre-treatment, III – sample after roughing, IV – sample after finishing

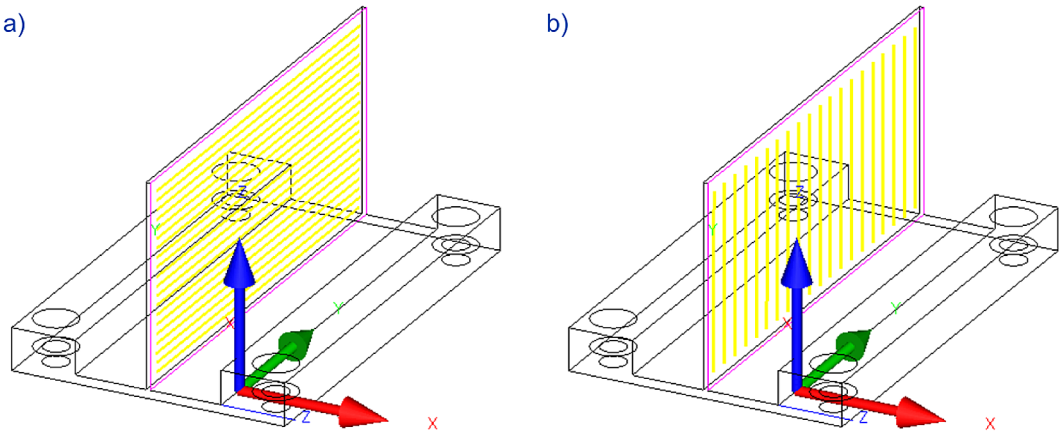


Figure 5. Visualization of Raster measurement strategy for: a) flatness deviation, b) wall thickness deviation (the second surface was measured using the same procedure to determine the wall thickness)

selection of the measurement procedure complied with Zeiss's guidelines, contained in the Cookbook user manual, which is a collection of best practices for performing coordinate measurements. The prepared measurement plan took into account recommendations regarding the selection of a datum reference frame, scanning technique, step size, scanning speed, and the evaluation of surface geometric features (including the use of filters).

RESULTS

First of all, the experimental results of flatness deviation (f_d) were analyzed from both quantitative and qualitative perspectives. An analysis of variance (ANOVA) was used to identify the regression model that provided the best fit for the flatness deviation results in a thin wall milled with a support insert versus the independent variables. The following models were considered: linear, two-factor interaction (2FI), quadratic, and cubic. The evaluation criteria included the sequential *p*-value, lack of fit *p*-value, as well as the adjusted R^2 and predicted R^2 coefficients. The linear and 2FI models were not statistically significant ($p > 0.05$) and, additionally, were characterized by negative values of the adjusted R^2 (-0.0051 and -0.1053) and the predicted R^2 (-0.6001 and -2.0762), indicating very poor agreement with the experimental results. In contrast, the third model (i.e., quadratic) proved to be highly statistically significant ($p < 0.0001$), with no significant lack of fit (lack of fit *p*-value = 0.1333). This model also achieved satisfactory values for the adjusted R^2 (0.9514) and the predicted R^2 (0.7936), confirming its accurate representation of the experimental data and acceptable predictive ability. Although the cubic model yielded a slightly higher adjusted R^2 value (0.9718), it also had a significantly lower value of the predicted R^2 (0.5470), indicating limited generalization ability for new observations. Based on the analysis, the quadratic response surface model was chosen as the most suited for further research, because it provided the best compromise between statistical significance, quality of fit, and predictive ability. Table 3 lists the statistical indicators describing the analyzed response surface models for thin-wall flatness deviation.

A statistical analysis of the quadratic response surface model results for thin-wall flatness deviation shows that the model's predictions fit the experimental data very well. The mean value of the analyzed variable is 0.1114 mm, with a small standard deviation of 0.0034 mm. The coefficient of variation of 3.07% indicates a slight dispersion of the results and high repeatability of the measurements. The high value of the coefficient of determination ($R^2 = 0.9717$) means that the model explains 97.17% of the variation in the data. Furthermore, the adjusted R^2 value of 0.9514 also confirms the model's very good fit, considering the number of parameters. The predicted R^2 value of 0.7936 indicates a satisfactory predictive ability of the model, although it is lower than the adjusted R^2 value, which may suggest certain limitations in predicting new observations. The adequate precision indicator reached a value of 20.6440, significantly going above the recommended threshold of 4, which demonstrates an adequate signal-to-noise ratio and confirms the

Table 3. Statistical indicators describing the tested response surface models for thin-wall flatness deviation

Model	Sequential *p*-value	Lack of fit *p*-value	Adjusted R^2	Predicted R^2
Linear	0.4123	0.0005	-0.0051	-0.6001
2FI	0.7662	0.0004	-0.1053	-2.0762
Quadratic	< 0.0001	0.1333	0.9514	0.7936
Cubic	0.1109	0.2393	0.9718	0.5470

model's appropriateness for research. Table 4 presents individual statistical parameters of this model for thin-wall flatness deviation.

A regression equation describing the effect of wall thickness (A) and cutting speed (B) on flatness deviation (f_d) was established using the coded variables (1):

$$f_d = 0.1236 - 0.0060A + 0.0065B + \\ + 0.0025AB + 0.0005A^2 - 0.0270B^2 \quad (1)$$

The developed quadratic model was validated using ANOVA, which confirmed its statistical significance (F-value of 47.99 and $p < 0.0001$), as well as described the effects of variables A and B on f_d in a thin wall milled with a support insert (Table 5). Among the analyzed parameters, both A and B were found to exert a considerable impact on the response value, yielding p-values amounting to 0.0035 and 0.0024. The interaction between the (AB) factors, however, proved to be statistically insignificant ($p = 0.1873$), which suggests that the effect of one parameter does not depend significantly on the level of the other. An analysis of the nonlinear terms showed that only the quadratic term related to B^2 had a significant effect on f_d ($F = 171.57$ and $p < 0.0001$). Conversely, the A^2 term was not statistically significant ($F = 0.0678$ and $p = 0.8020$). This indicates that the nonlinear relationship occurs primarily with respect to B. The lack-of-fit test was also an important element in assessing the model's quality. The obtained p-value of 0.1333, which is higher than the accepted significance level of 0.05, shows the absence of a statistically significant lack of fit between the model and the experimental data. Summing up, it means that the developed regression equation accurately describes the relationships within the studied range of parameters and can be used to analyze and predict f_d in a thin wall manufactured using a silicone casting resin support insert.

Figure 6 shows the response surface plot describing the relationship between the A and B variables and f_d in a thin wall milled with a support insert. An analysis of the plot reveals that both process parameters significantly affect the response, although their effects vary. As v_c is increased from 300 to $v_c \approx$ 600–700 m/min, the flatness deviation increases, reaching its maximum at the mid-range speeds ($v_c \approx$ 600–700 m/min). At higher cutting speeds, a decreasing trend in flatness deviation was observed; thus, it can be concluded that the results obtained at $v_c = 900$ m/min are comparable to those obtained at $v_c = 300$ m/min. This trend confirms the significance of the quadratic term of cutting speed, as shown in the ANOVA. The impact of wall thickness is less pronounced; however, increasing wall thickness resulted in progressively lower flatness deviation values. The highest flatness deviation values were predicted at $t = 1$ mm and $v_c \approx$ 600–700 m/min. In contrast, the smallest flatness deviations were obtained for $t = 2$ mm and $v_c = 300$ m/min or $v_c = 900$ m/min. At the same time, the lack of a pronounced surface twist suggests the minor influence of interactions between the analyzed variables, which is consistent with the ANOVA results, in which the AB interaction term was not statistically significant.

Figure 7 presents the interaction plots describing the impact of A and B on f_d in a thin wall. The solid lines represent the values predicted by the regression model, while the shaded areas and dashed lines denote the confidence intervals.

Table 4. Statistical indicators of a model for thin-wall flatness deviation

Standard deviation [mm]	Mean [mm]	Coefficient of variation [%]	Coefficient of determination R^2 [-]	Adjusted R^2 [-]	Predicted R^2 [-]	Adequate precision [-]
0.0034	0.1114	3.07	0.9717	0.9514	0.7936	20.6440

Table 5. ANOVA results of a model for thin-wall flatness deviation

Source	Sum of squares	Degrees of freedom	Mean square	*F*-value	*p*-value	
Model	0.0028	5	0.0006	47.99	< 0.0001	significant
A-Wall thickness	0.0002	1	0.0002	18.56	0.0035	
B-Cutting speed	0.0003	1	0.0003	21.55	0.0024	
AB	< 0.0001	1	< 0.0001	2.14	0.1873	
A^2	7.941×10^{-7}	1	7.941×10^{-7}	0.0678	0.8020	
B^2	0.0020	1	0.0020	171.57	< 0.0001	
Residual	0.0001	7	< 0.0001			
Lack of fit	0.0001	3	< 0.0001	3.41	0.1333	not significant
Pure error	< 0.0001	4	5.753×10^{-6}			
Cor total	0.0029	12				

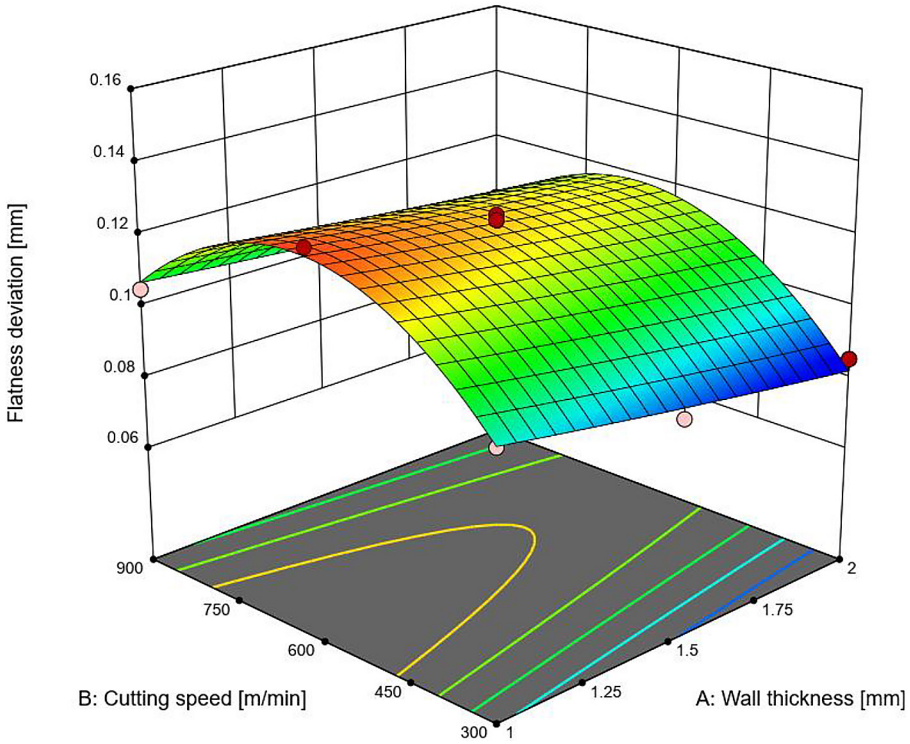


Figure 6. Response surface plot for thin-wall flatness deviation

Figure 7a plots the relationship between f_d and A for two extreme B (black line: v_c = 300 m/min, red line: v_c = 900 m/min). For both analyzed cutting speeds, one can observe a trend of decreasing flatness deviation with increasing wall thickness, although this change is slightly more pronounced at the lower cutting speed (v_c = 300 m/min). At the same time, the shape of both curves is similar, and their slopes remain comparable throughout the analyzed range. The fact that the lines do not intersect and run nearly parallel indicates that the effect of thickness on this deviation is similar, regardless of the cutting speed. Figure 7b shows the variation in f_d as a function of B for different A (black line: t = 1 mm, red line: t = 2 mm). For all analyzed wall thicknesses, the curves exhibit similar patterns, characterized by an increase in the flatness deviation to a maximum value reached at $v_c \approx$ 600–700 m/min, followed by a drop in this parameter as the cutting speed continues to increase. The resulting data confirm the significant effect of the quadratic term of cutting speed, as previously demonstrated in the analysis of variance. No clear differences between the

slopes of individual curves can be observed in either plot, indicating minor interaction between the wall thickness and the cutting speed. This observation is confirmed by the ANOVA results, where the *AB* interaction term is not statistically significant (p = 0.1873). This means that the effect of both parameters on flatness deviation can be considered largely independently. Figures 8–10 show the 3D visualization of f_d versus A (t = 1–2 mm, with a step of 0.5 mm) and B (v_c =

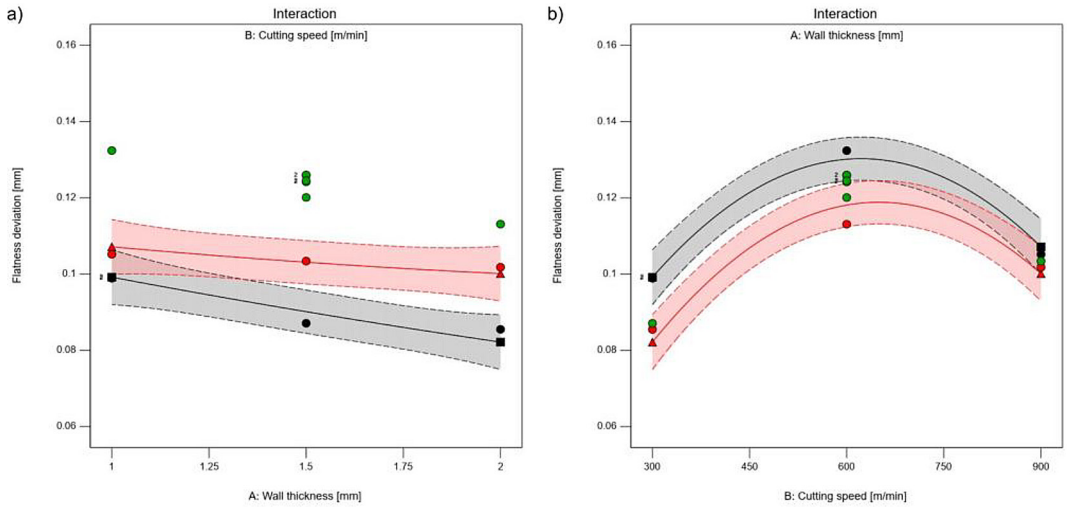


Figure 7. Interaction plots of thin wall flatness deviation: a) A versus B (black line: v_c = 300 m/min, red line: v_c = 900 m/min), b) B versus A (black line: t = 1 mm, red line: t = 2 mm)

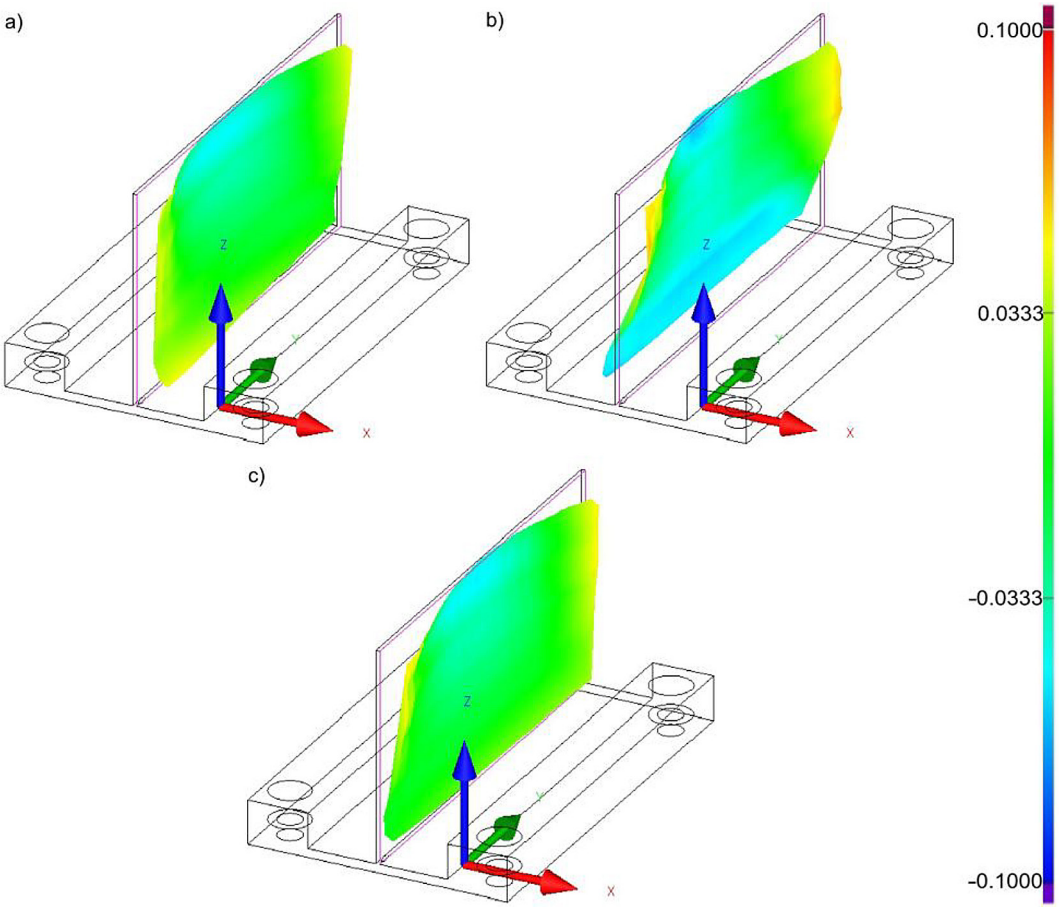


Figure 8. 3D visualization of flatness deviation for t = 1 mm: a) v_c = 300 m/min, b) v_c = 600 m/min, c) v_c = 900 m/min

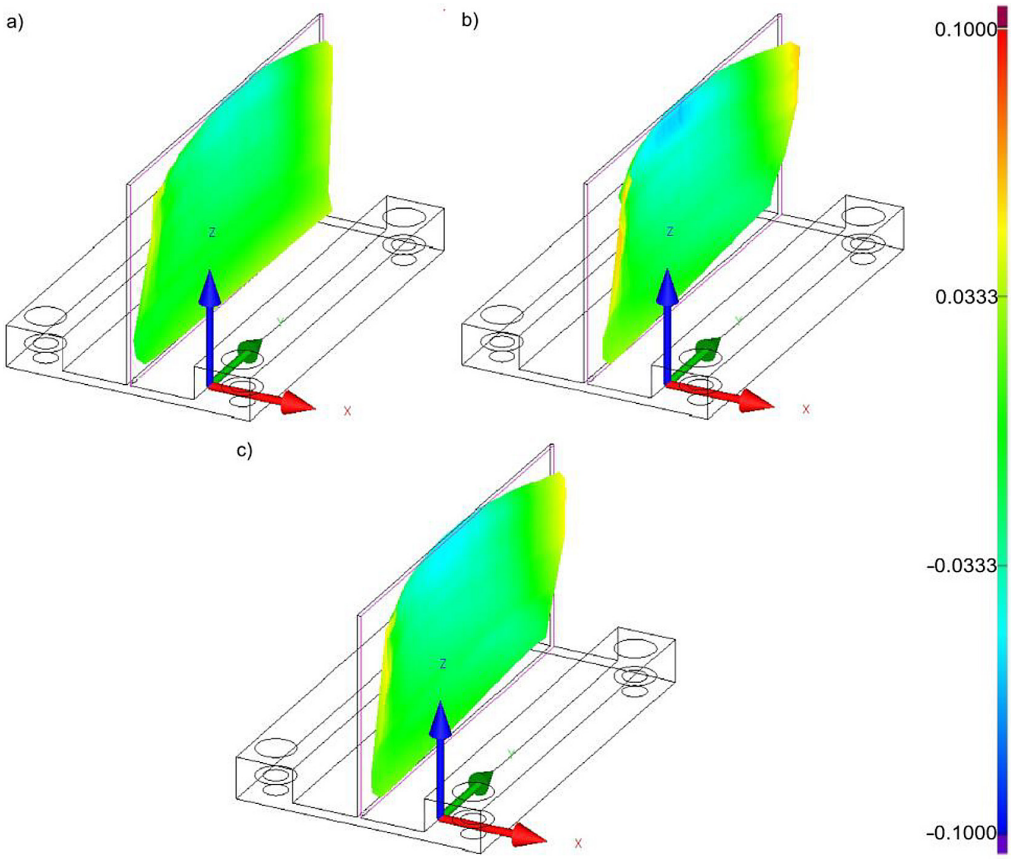


Figure 9. 3D visualization of flatness deviation for t = 1.5 mm: a) v_c = 300 m/min, b) v_c = 600 m/min, c) v_c = 900 m/min

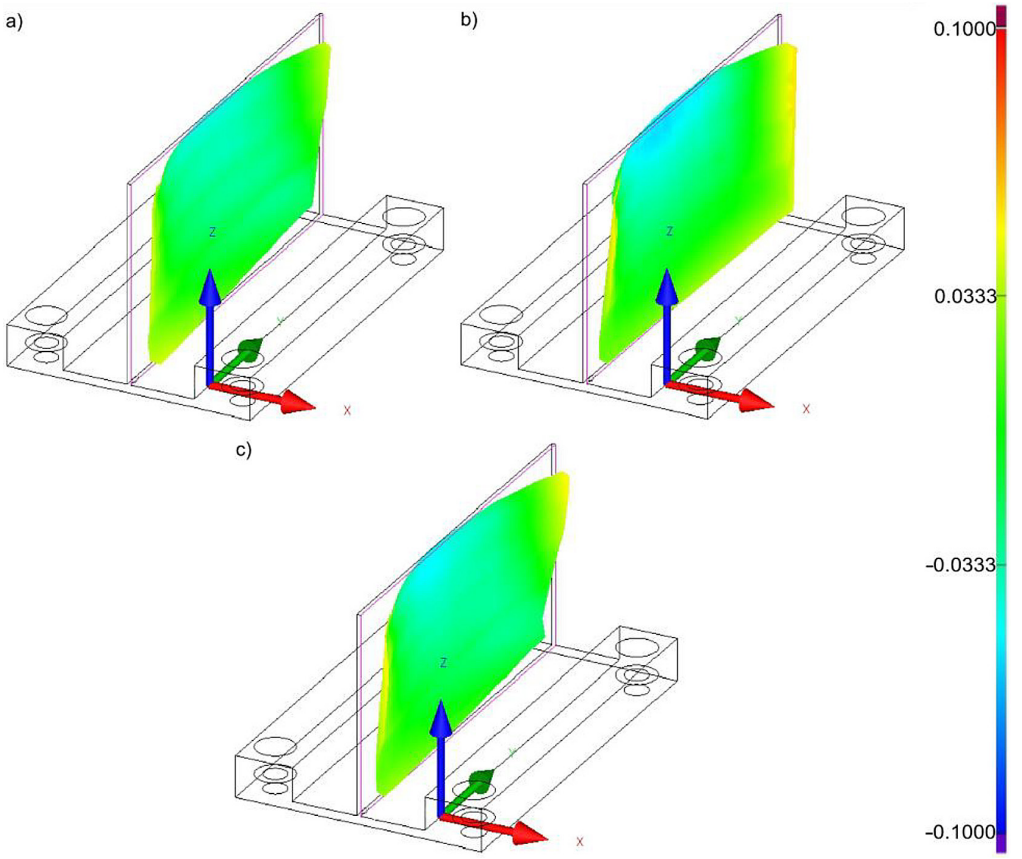


Figure 10. 3D visualization of flatness deviation for t = 2 mm: a) v_c = 300 m/min, b) v_c = 600 m/min, c) v_c = 900 m/min

300–900 m/min, with a step of 300 m/min). The results were used to assess the post-machining deformation in the thin wall. The idealized reference plane is marked in pink in the visualizations. A similar pattern of deformation was observed for all cases. The greatest deviations from the nominal geometry occurred in the top part of the wall, particularly in the areas close to the wall's edges, which indicates that these areas are more susceptible to deformation. A comparison of the individual variants showed that the most favorable effects of milling with a support insert were obtained for t = 2 mm and v_c = 300 m/min; however, the differences between the thinnest and the thickest walls are negligible. Similar observations were made for the extreme cutting speeds. Additionally, no marks running perpendicular to the direction of feed were observed, the presence of which could indicate chatter and instability of the cutting process.

Figure 11 compares f_d in a thin wall that was milled with and without a support insert. After machining without a support insert (Figure 11a), significant deformation of the thin-walled surface and evident chatter marks can be observed, resulting from the low stiffness of the workpiece wall during milling at a maximized depth of cut. The use of a support insert (Figure 11b) significantly reduces wall deformation while simultaneously eliminating characteristic signs of chatter. Research on full-height milling of a thin wall without a support insert was described in the earlier studies [42,43]. These studies served as a starting point for further research aimed at finding a solution to improve the dimensional and geometric accuracy of the wall.

The second aspect of this study was wall thickness deviation, i.e., the other parameter used to assess the post-machining deformation in the tested wall. The analysis began with selecting the most appropriate regression model from among the following: linear, with two-factor interactions (2FI), quadratic, and cubic. The linear model was characterized by a low value (adjusted R^2 = 0.1516) and a negative predicted R^2 value (-0.4047), indicating a limited ability to describe and predict the response. The inclusion of two-factor interactions did not improve the fit, as confirmed by even lower values of the adjusted R^2 (0.0589) and the predicted R^2 (-2.0394). A significant improvement in the statistical parameters was observed for the quadratic model, which showed a high statistical significance (p = 0.0001) with no significant lack of fit (lack of fit p-value = 0.1480). The adjusted R^2 value (0.9117) indicated that the model fit the experimental data very well, while the predicted R^2 value (0.6092) confirmed its acceptable predictive ability. Although the cubic model was characterized by higher values of the adjusted R^2 (0.9633) and the predicted R^2 (0.9776), it was not selected for further analysis because it was classified as an aliased model, which prevents the unambiguous estimation of all coefficients. Therefore, the quadratic model was found to be the most suitable for further research. Table 6 lists all statistical parameters of the tested response surface models for thin-wall thickness deviation.

The quality of fit of the quadratic response surface model describing thin-wall thickness deviation was assessed based on the detailed statistical parameters listed in Table 7. The mean value of the

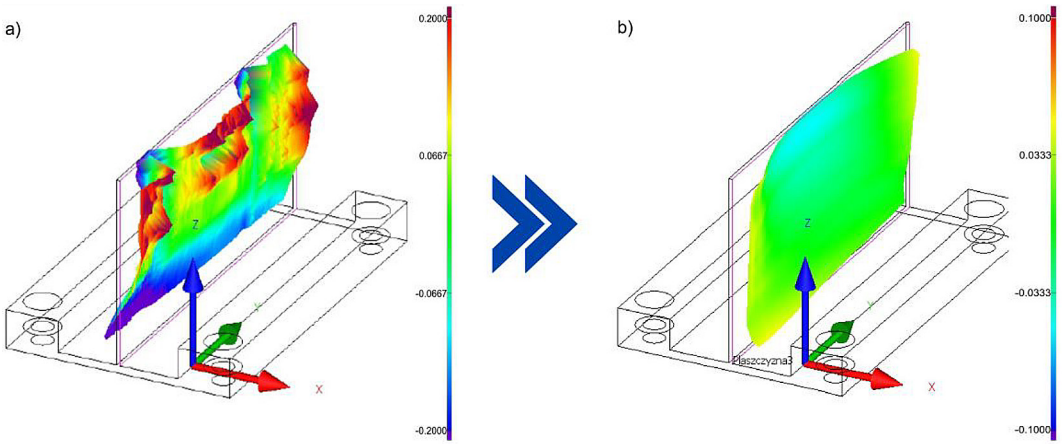


Figure 11. Comparison of flatness deviation in a thin wall milled at a maximized depth of cut: a) without a support insert [42], b) with a support insert

analyzed variable was 0.1482 mm. The relatively low values of both the standard deviation (0.0057 mm) and the coefficient of variation (3.82%) indicate good repeatability of the obtained results. The developed model yielded a high value of the coefficient of determination ($R^2 = 0.9485$), which means that it accounted for 94.85% of the total variation in wall thickness deviation. At the same time, the high value of the adjusted R^2 (0.9117) confirmed the model's adequacy, given the number of parameters and degrees of freedom. These values demonstrate the high quality of the studied phenomenon's description produced by the model. On the other hand, the predicted R^2 value was 0.6092, demonstrating the model's satisfactory predictive ability with respect to new observations. This may suggest a partial overfitting of the model or the model's limited ability to generalize the results beyond the range of data used to build it. For this reason, the predicted results should be approached with caution, especially when extrapolating them beyond the analyzed experimental range. In addition, the adequate precision value of 15.8941 is significantly above the recommended threshold of 4. This indicates a favorable signal-to-noise ratio. The model was therefore considered adequate for subsequent response surface analysis.

Next, the dependence of thin wall thickness deviation (t_d) on wall thickness (A) and cutting speed (B) was represented by the following regression equation formulated using coded variables (2):

$$t_d = 0.1629 - 0.0141A + 0.0038B + \\ + 0.0012AB - 0.0039A^2 - 0.0280B^2 \quad (2)$$

The ANOVA results prove that the quadratic model describing the relationship between t_d and the variables A and B is statistically significant (Table 8). This is confirmed by the F-statistic value of 25.79 and the corresponding probability level of $p = 0.0002$. The results indicate that the model reliably captures the impact of the analyzed independent variables on the tested response. Among the analyzed factors, A had a considerable impact on t_d, with an F-value of 37.12 and a p-value of 0.0005. This means that changes in A significantly affect the analyzed response. The quadratic effect of B^2 also proved to be significant, producing the highest F-statistic value (67.61) and a p-value of < 0.0001. This points to the nonlinear nature of the effect of B on t_d of the tested component. In contrast, the linear effect of B was not statistically significant ($p = 0.1438$), nor was the AB interaction, yielding $p = 0.6964$. The quadratic effect of the wall thickness (A^2) was also found to be statistically insignificant ($p = 0.2918$). The results demonstrate that t_d primarily depends on A and the nonlinear effect of B, while the remaining model components have limited statistical significance. The lack-of-fit analysis produced a p-value of 0.1480 (for $\alpha = 0.05$). This means that this equation adequately captures the relationships present in the analyzed process. Thus, this model can be considered a reliable tool for describing and predicting thin-wall thickness deviation in parts manufactured using a support insert, within the examined range of parameters.

The effect of A and B on the thin-wall t_d is visualized as a three-dimensional response surface plot (Figure 12). The results show a nonlinear dependence of the measured response on cutting speed. Increasing the cutting speed in the range from $v_c = 300$ to approximately $v_c \approx 600$ m/min caused an increase in the thickness

Table 6. Statistical indicators describing the analyzed response surface models for thin wall thickness deviation

Model	Sequential *p*-value	Lack of fit *p*-value	Adjusted R^2	Predicted R^2
Linear	0.1767	0.0027	0.1516	-0.4047
2FI	0.9036	0.0020	0.0589	-2.0394
Quadratic	0.0001	0.1480	0.9117	0.6092
Cubic	0.0481	0.9939	0.9633	0.9776

Table 7. Statistical indicators of a model for thin-wall thickness deviation

Standard deviation [mm]	Mean [mm]	Coefficient of variation [%]	Coefficient of determination R^2 [-]	Adjusted R^2 [-]	Predicted R^2 [-]	Adequate precision [-]
0.0057	0.1482	3.82	0.9485	0.9117	0.6092	15.8941

Table 8. ANOVA results of a model for thin-wall thickness deviation

Source	Sum of squares	Degrees of freedom	Mean Square	*F*-value	*p*-value	
Model	0.0041	5	0.0008	25.79	0.0002	significant
A-Wall thickness	0.0012	1	0.0012	37.12	0.0005	
B-Cutting speed	0.0001	1	0.0001	2.71	0.1438	
AB	5.290×10^{-6}	1	5.290×10^{-6}	0.1654	0.6964	
A^2	< 0.0001	1	< 0.0001	1.30	0.2918	
B^2	0.0022	1	0.0022	67.61	< 0.0001	
Residual	0.0002	7	< 0.0001			
Lack of fit	0.0002	3	0.0001	3.16	0.1480	not significant
Pure error	0.0001	4	< 0.0001			
Cor total	0.0043	12				

deviation, whereas exceeding this cutting speed limit resulted in a decrease in the thickness deviation. This was confirmed by the significance of the quadratic term for cutting speed in the ANOVA. The impact of wall thickness was also noticeable, but it was linear. As the wall thickness increased, the thickness deviation gradually decreased. It should be added that the impact of the wall thickness also increased with increasing the cutting speed. At higher cutting speeds, the differences in wall thickness deviation among the analyzed wall thickness variants became more pronounced, which indicates the increasing significance of the workpiece's stiffness. The highest values of the analyzed response were produced with t = 1 mm and $v_c \approx$ 600 m/min, while the smallest deviations were obtained for t = 2 mm and v_c = 300 m/min or v_c = 900 m/min. The limited impact of interactions between the analyzed factors was also confirmed by the regular and nearly parallel pattern of the contour lines, indicating the dominance of main effects.

Figure 13 shows interaction plots illustrating the effect of wall thickness and cutting speed on the thin wall thickness deviation. As in the flatness deviation plot, the solid lines represent the

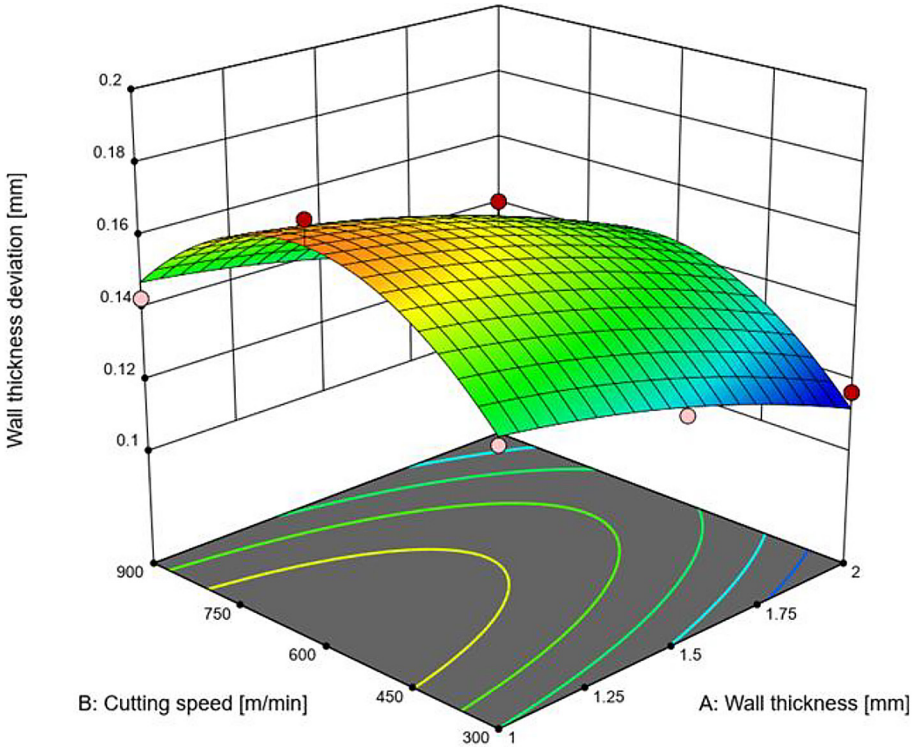


Figure 12. Response surface plot for thin-wall thickness deviation

values predicted by the regression model, while the shaded areas bounded by dashed lines represent the 95% confidence intervals. The variation in thin wall thickness deviation as a function of the wall thickness for two extreme cutting speeds (black line: v_c = 300 m/min, red line: v_c = 900 m/min) is shown in Figure 13a. For both cases, a gradual decrease in the measured deviation is observed as the wall thickness is increased. This trend is similar for both tested cutting speeds, although the decrease in the response value is slightly more pronounced at the lower speed. The parallel behavior pattern of the curves and the nearly constant difference between them indicate that the effect of wall thickness remains similar, whatever the cutting speed. Figure 13b, in turn, shows a relationship between the thickness deviation and the cutting speed for two extreme thickness values (black line: t = 1 mm, red line: t = 2 mm). In both cases, the curves exhibit nonlinear behavior. As the cutting speed is increased in the range of v_c = 300–600 m/min, the thickness deviation increases, reaching its maximum value at v_c = 600 m/min, and then decreases as the speed continues to rise up to 900 m/min. This relationship indicates a quadratic effect of cutting speed, which agrees with the ANOVA results. Neither plot shows any profound changes in the relative positions or slopes of the analyzed curves. The absence of intersection and the similar behavior across the entire range of the examined parameters suggest a weak interaction between wall thickness and cutting speed. This conclusion agrees with the results of the ANOVA analysis, where the *AB* interaction term was not statistically significant, meaning that the influence of both factors on the thickness deviation can largely be analyzed independently.

Based on these results, both wall thickness and cutting speed were found to significantly influence post-machining deformation in thin walls that were milled with a support insert at a maximized axial depth of cut.

DISCUSSION

The findings demonstrate that using a support insert made of a silicone casting resin is an effective method for reducing post-machining deformation in thin walls that are finish milled at a maximized axial depth of cut. This is particularly important in the manufacture of aerospace components, where maintaining high dimensional and geometric accuracy is a key technological challenge.

The statistical analysis has shown that the flatness and wall thickness deviations are affected by two independent variables under study, namely wall thickness and cutting speed. A greater thickness of the wall entailed reduced post-machining deformation, which is associated with an increase in the stiffness of the workpiece. Furthermore, a nonlinear effect of the cutting speed was observed. Taking into account the response surfaces obtained, the maximum values of the examined deviations were recorded at the mid-range speeds (v_c ≈ 600–700 m/min), while

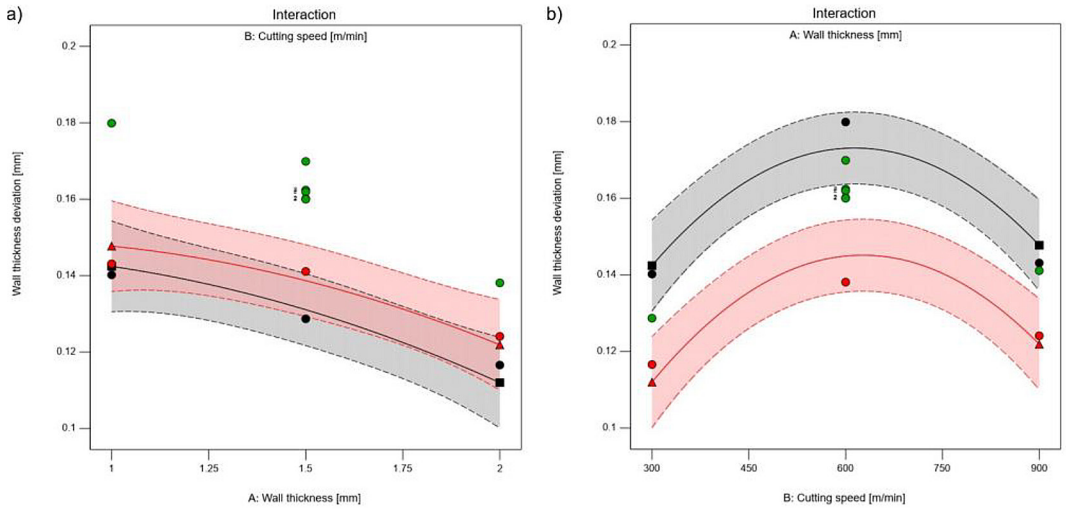


Figure 13. Interaction plots of thin wall thickness deviation: a) *A* versus *B* (black line: v_c = 300 m/min, red line: v_c = 900 m/min), b) *B* versus *A* (black line: t = 1 mm, red line: t = 2 mm)

lower deviation values were obtained at both v_c = 300 m/min and v_c = 900 m/min. Regarding the maximum cutting speed tested, this phenomenon may have been related to the high-speed cutting (HSC). According to the authors of [30], this method implies a decrease in cutting force and a reduction in tool-workpiece contact time. In addition, HSC is associated with a more favorable chip formation process and a more uniform distribution of loads acting on the workpiece, which helps maintain the dimension- and geometry-related accuracy of manufactured parts. At the same time, it should be noted that such conditions may promote the occurrence of dynamic phenomena, as confirmed by [56].

Importantly, it should be stressed that the macroscopic examination of the thin wall surfaces and 3D visualizations of their flatness deviations did not reveal any characteristic signs of chatter on the machined surfaces. This indication suggests that the use of the support insert may have increased the local rigidity of the workpiece-tool system, thus limiting the occurrence of chatter [57]. However, it should be emphasized that no direct dynamic measurements, such as vibration or cutting force measurements, along with frequency-domain vibration analysis, were performed to independently verify the occurrence or absence of chatter [19]. Therefore, the obtained results should be interpreted as an indication of the lack of visible or geometrically detectable manifestations of chatter under the investigated machining conditions, rather than as definitive evidence of its complete absence. Further studies incorporating direct vibration and cutting force measurements are required to quantitatively assess the dynamic stability of the machining process and to confirm the influence of the support insert on chatter suppression. The study could also be supplemented with an analysis of surface roughness, another indicator that may be associated with the occurrence of chatter during the machining process [58]. The negligible significance of the wall thickness and cutting speed interaction indicates that the effect of either variable on the post-machining deformation is only slightly dependent on the level of the other factor. From a technological standpoint, this situation is advantageous because it facilitates process optimization. The cutting speed can be selected independently of changes in the geometry of the workpiece, without the risk of a sudden change in the quality of manufactured parts.

Particularly interesting conclusions emerge from comparing these results with the findings of the author's earlier studies on thin wall milling in workpieces having the same geometry, but without the use of a support insert [42,43]. Previous experiments conducted under comparable conditions, including the same cutting tool and machining parameters, enabled the effect of the support insert on thin-wall deformation to be assessed. The studies demonstrated that the occurrence of chatter marks and a significant deterioration in part accuracy practically ruled out the use of v_c = 900 m/min. The best (though not ideal) machining results were primarily obtained at v_c = 300 m/min, while at higher cutting speeds, one could observe increased process instability and reduced part quality. The results reported in this work demonstrate that the use of a support insert fundamentally changes the nature of the process. Despite a threefold increase in the cutting speed to v_c = 900 m/min, no deterioration in the machined surface accuracy or characteristic chatter marks were observed. This suggests that the insert effectively increases the dynamic rigidity of the machining system, enabling the machining process under high-speed cutting (HSC) conditions [30,59]. This finding is particularly significant from the perspective of industrial applications, as increasing the speed value from v_c = 300 m/min to v_c = 900 m/min entails that the time required for the finishing operation can be reduced by approximately a factor of three. In terms of mass production of aerospace components, this directly translates into increased process efficiency and reduced manufacturing costs while maintaining the accurate dimensions and geometry.

It must also be highlighted that in the previous studies [42,43], the use of the maximum depth of cut for milling a thin-walled component with the dimensions h = 48 mm and t = 1 mm was impossible due to the insufficient stiffness of the workpiece and the occurrence of considerable deformation and chatter marks, which are the main problems resulting from the machining of such parts [17,60]. However, the use of a support insert enabled effective machining of a workpiece with such geometry, which confirms the high effectiveness of the developed solution in terms of increasing the machinability of thin-walled components. Thus, the proposed support insert not only reduces post-machining deformation but also expands the range of machining parameters that can be employed in high-performance

milling of thin-walled elements. The simplicity and relatively low cost of the proposed insert are also noteworthy. Unlike conventional metal supports [22,28], this solution allows for a more uniform distribution of contact pressures across the wall surface and effective vibration damping. The findings suggest that the insert material not only increases the system's stiffness but also acts as a damping element.

From a broader perspective, this study aligns with the current trend toward the development of machining methods for thin-walled parts. As the demands of the aerospace industry increase, it is becoming necessary to seek the solutions that reduce machining time without compromising product quality. The developed support method may provide a practical solution for achieving this goal.

CONCLUSIONS

The main outcomes of the conducted research are summarized as follows:

1. The use of a support insert during finish milling at a maximized axial depth of cut effectively reduced the post-machining deformation in a thin wall. The results demonstrated that the additional support reduced the workpiece's susceptibility to deflection induced by the cutting force and probably improved the stability of the milling process.
2. The statistical analysis confirmed that the tested independent variables had a considerable influence on the values of the response deviations, i.e., flatness and wall thickness. A linear effect was observed for the wall thickness, while a nonlinear effect was observed for the cutting speed.
3. The wall thickness increase led to reduced post-machining deformation, which resulted from the higher stiffness of the workpiece and, consequently, from its reduced susceptibility to cutting force-induced deflection.
4. The highest values of the analyzed deviations were produced with the mid-range cutting speeds ($v_c \approx$ 600–700 m/min), while the extreme speeds v_c = 300 m/min and v_c = 900 m/min yielded higher manufacturing accuracy of the parts.
5. No significant interactions were established between the wall thickness and the cutting speed, demonstrating that the influence of these two variables on post-machining deformation could be investigated independently. This means that the influence of one variable remains similar throughout the entire range of the values of the other variable.
6. The macroscopic examination and 3D visualizations of the flatness deviation did not reveal any characteristic signs of chatter, suggesting that the dynamic stiffness of the system was effectively increased thanks to the use of a support insert. It should be emphasized that the absence of characteristic chatter-related features was not directly verified using vibration or cutting force measurements. Therefore, this finding should be regarded as an indication based on the investigated surface and geometric characteristics rather than as conclusive evidence of dynamic stability.
7. A comparison of the results obtained from this research with the findings of earlier studies that were conducted without the use of a support insert revealed that the support insert significantly expanded the range of machining parameters that could be used in thin-wall milling. In particular, the support insert enabled the stable machining process at v_c = 900 m/min, which was previously impossible due to chatter marks.
8. The use of a support insert increased the machinability of thin-walled elements, thus enabling the machining of workpieces with very low stiffness, such as open walls with the dimensions h = 48 mm and t = 1 mm, which would have been impossible to machine without additional support. From an industrial perspective, this creates an opportunity to significantly increase process efficiency, because increasing the cutting speed from v_c = 300 m/min to v_c = 900 m/min can lead to a roughly threefold reduction in the time required for the finishing operation.
9. The study has shown that the use of a support insert made of a silicone casting resin is a promising solution for machining thin-walled components by finish milling at a maximized axial depth of cut. The results confirm the solution's ability to effectively reduce post-machining deformation while maintaining high process efficiency, which is vital in the manufacture of parts for the aerospace and defense industries.

Acknowledgements

This publication is a result of the project entitled "Development of the milling technique of thin-walled integral elements made of aviation light metal alloys in the context of minimalisation post-machining deformations", contract number: LIDER14/0153/2023, total project value: 1,543,750.00 PLN. The project is financed by the National Centre for Research and Development under the 14th edition of the LIDER Programme.

REFERENCES

1. Del Sol I, Rivero A, de Lacalle LNL, Gamez AJ. Thin-wall machining of light alloys: A review of models and industrial approaches. Materials. 2019;12:2012. https://doi.org/10.3390/ma12122012
2. Bałon P, Rejman E, Świątoniowski A, Kiełbasa B, Smusz R, Szostak J, et al. Thin-walled integral constructions in aircraft industry. Procedia Manuf. 2020;47:498–504. https://doi.org/10.1016/j.promfg.2020.04.153
3. Lu W, Zong C, Ni C, Yu X, Liu D. Study on the surface integrity of 7050 aluminum alloy with different crystal orientations during high-speed machining. Int J Adv Manuf Technol. 2023;125:661–78. https://doi.org/10.1007/s00170-022-10717-y
4. Lin S, Zhao Z, Fu Y. Flexible registration strategy for optimizing machining allowance of thin-walled parts. Measurement. 2024;238:115326. https://doi.org/10.1016/j.measurement.2024.115326
5. Liu H, Wang C, Li T, Bo Q, Liu K, Wang Y. Fixturing technology and system for thin-walled parts machining: a review. Front Mech Eng. 2022;17:55. https://doi.org/10.1007/s11465-022-0711-5
6. Wang J, Zhang D, Wu B, Luo M. Prediction of distortion induced by machining residual stresses in thin-walled components. Int J Adv Manuf Technol. 2018;95:4153–62. https://doi.org/10.1007/s00170-017-1358-y
7. Ma Y, Zhang J, Yu D, Feng P, Xu C. Modeling of machining distortion for thin-walled components based on the internal stress field evolution. Int J Adv Manuf Technol. 2019;103:3597–612. https://doi.org/10.1007/s00170-019-03736-9
8. Li X, Liu J, Wu H, Miao K, Wu H, Li R, et al. Research progress of residual stress measurement methods. Heliyon. 2024;10:e28348. https://doi.org/10.1016/j.heliyon.2024.e28348
9. Llanos I, Aurrekoetxea M, Agirre A, López De Lacalle LN, Zelaieta O. On-machine characterization of bulk residual stresses on machining blanks. Procedia CIRP. 2019;82:406–10. https://doi.org/10.1016/j.procir.2019.04.012
10. Radu P, Schnakovszky C. A review of proposed models for cutting force prediction in milling parts with low rigidity. Machines. 2024;12:140. https://doi.org/10.3390/machines12020140
11. Akhtar W, Lazoglu I, Liang SY. Prediction and control of residual stress-based distortions in the machining of aerospace parts: A review. J Manuf Process. 2022;76:106–22. https://doi.org/10.1016/j.jmapro.2022.02.005
12. Jiang X, Wang Y, Ding Z, Li H. An approach to predict the distortion of thin-walled parts affected by residual stress during the milling process. Int J Adv Manuf Technol. 2017;93:4203–16. https://doi.org/10.1007/s00170-017-0811-2
13. Chen Z, Qian L, Cui R, Liu J, Zhang Q. Machining-induced residual stress analysis and multi-objective optimization for milling process of Mg–Li alloy. Measurement. 2022;204:112127. https://doi.org/10.1016/j.measurement.2022.112127
14. Weber D, Kirsch B, D'Elia CR, Linke BS, Hill MR, Aurich JC. Simulation-Based Investigation of the Distortion of Milled Thin-Walled Aluminum Structural Parts Due to Residual Stresses. Proc 3rd Conf Phys Model Virtual Manuf Syst Process. Cham: Springer International Publishing; 2023. p. 149–69. https://doi.org/10.1007/978-3-031-35779-4_9
15. Cerutti X, Mocellin K. Influence of the machining sequence on the residual stress redistribution and machining quality: Analysis and improvement using numerical simulations. Int J Adv Manuf Technol. 2016;83:489–503. https://doi.org/10.1007/s00170-015-7521-4
16. Huang X, Sun J, Li J. Effect of initial residual stress and machining-induced residual stress on the deformation of aluminium alloy plate. Stroj Vestn - J Mech Eng. 2015;61:131–7. https://doi.org/10.5545/sv-jme.2014.1897
17. Wu G, Li G, Pan W, Raja I, Wang X, Ding S. A state-of-art review on chatter and geometric errors in thin-wall machining processes. J Manuf Process. 2021;68:454–80. https://doi.org/10.1016/j.jmapro.2021.05.055
18. Zhang X, Wan L, Ran X. Research progress on the chatter stability in machining systems. Int J Adv Manuf Technol. 2024;131:29–62. https://doi.org/10.1007/s00170-024-13050-8
19. Korpysa J, Zagórski I. Vibration analysis during AZ31 magnesium alloy milling with the use of different toolholder types. Eksploat i Niezawodn – Maint Reliab. 2022;24:489–501. https://doi.org/10.17531/ein.2022.3.10
20. Zagórski I, Weremczuk A, Kulisz M, Skoczylas A. Vibration and stability in dry rough milling AZ31B magnesium alloy using end mills with different edge geometry. Measurement. 2025;256:118523. https://

doi.org/10.1016/j.measurement.2025.118523

21. Bachrathy D, Kiss AK, Kossa A, Berezvai S, Hajdu D, Stepan G. In-process monitoring of changing dynamics of a thin-walled component during milling operation by ball shooter excitation. J Manuf Mater Process. 2020;4:78. https://doi.org/10.3390/jmmp4030078
22. Li X, Ni J, Liu X, Yue C, Yang S, Ji X, et al. Chatter-free milling of aerospace thin-walled parts. J Mater Process Technol. 2025;341:118903. https://doi.org/10.1016/j.jmatprotec.2025.118903
23. Zheng Y, Zhao Z, Xu B, Yu Y, Xu J. A method to predict chatter stability accurately in milling thin-walled parts by considering force-induced deformation. J Manuf Process. 2023;106:552–63. https://doi.org/10.1016/j.jmapro.2023.10.033
24. Zawada-Michałowska M, Pieśko P. Analysis of machining strategies in terms of residual stress and post-machining deformation of thin-walled element. Int J Adv Manuf Technol. 2026;142:2335–58. https://doi.org/10.1007/s00170-025-17176-1
25. Wang J, Ibaraki S, Matsubara A. A cutting sequence optimization algorithm to reduce the workpiece deformation in thin-wall machining. Precis Eng. 2017;50:506–14. https://doi.org/10.1016/j.precisioneng.2017.07.006
26. Kurpiel S, Cudok B, Zagórski K, Cieślik J, Skrzypkowski K, Brostow W. Influence of tools and cutting strategy on milling conditions and quality of horizontal thin-wall structures of titanium alloy Ti6Al4V. Sensors. 2023;23:9905. https://doi.org/10.3390/s23249905
27. Lukic D, Cep R, Vukman J, Antic A, Djurdjev M, Milosevic M. Multi-criteria selection of the optimal parameters for high-speed machining of aluminum alloy AL7075 thin-walled parts. Metals. 2020;10. https://doi.org/10.3390/met10121570
28. Li Z, Zeng Z, Yang Y, Ouyang Z, Ding P, Sun J, et al. Research progress in machining technology of aerospace thin-walled components. J Manuf Process. 2024;119:463–82. https://doi.org/10.1016/j.jmapro.2024.03.111
29. Lassila AA, Svensson D, Wang W, Andersson T. Numerical evaluation of cutting strategies for thin-walled parts. Sci Rep. 2024;14:1459. https://doi.org/10.1038/s41598-024-51883-1
30. Bałon P, Rejman E, Smusz R, Szostak J, Kiełbasa B. Implementation of high speed machining in thin-walled aircraft integral elements. Open Eng. 2018;8:162–9. https://doi.org/10.1515/eng-2018-0021
31. Li W, Wang L, Yu G. Force-induced deformation prediction and flexible error compensation strategy in flank milling of thin-walled parts. J Mater Process Technol. 2021;297:117258. https://doi.org/10.1016/j.jmatprotec.2021.117258
32. Liu G, Wang Y, Huang B, Ding W. The intelligent monitoring technology for machining thin-walled components: A review. Machines. 2024;12:876. https://doi.org/10.3390/machines12120876
33. Zhu J, Liu X, Peng H, Liu W, Li Z. Exploration of cutting processing mode of low-rigidity parts for intelligent manufacturing. Micromachines. 2025;16:624. https://doi.org/10.3390/mi16060624
34. Liang J, Wu D, Wang H, Zhang H, Zhou F, Xu L. Chatter suppression in thin-walled part machining via conformal flexible clamping. Int J Mech Sci. 2025;305:110747. https://doi.org/10.1016/j.ijmecsci.2025.110747
35. Liu C, Sun J, Li Y, Li J. Investigation on the milling performance of titanium alloy thin-walled part with air jet assistance. Int J Adv Manuf Technol. 2018;95:2865–74. https://doi.org/10.1007/s00170-017-1420-9
36. Fei J, Lin B, Xiao J, Ding M, Yan S, Zhang X, et al. Investigation of moving fixture on deformation suppression during milling process of thin-walled structures. J Manuf Process. 2018;32:403–11. https://doi.org/10.1016/j.jmapro.2018.03.011
37. Wan M, Dang X-B, Zhang W-H, Yang Y. Chatter suppression in the milling process of the weakly-rigid workpiece through a moving fixture. J Mater Process Technol. 2022;299:117293. https://doi.org/10.1016/j.jmatprotec.2021.117293
38. Liu H, Wang J, Luo Q, Bo Q, Li T, Wang Y. Effect of controllable magnetic field-induced MRF solidification on chatter suppression of thin-walled parts. Int J Adv Manuf Technol. 2020;109:2881–90. https://doi.org/10.1007/s00170-020-05783-z
39. Leksycki K, Kaczmarek-Pawelska A. Surface topography and corrosion resistance of AISI 630 stainless steel after finish turning under different cooling methods. J Manuf Process. 2024;124:1249–58. https://doi.org/10.1016/j.jmapro.2024.07.026
40. Lisowicz J, Krupa K, Leksycki K, Rusinek R, Wojciechowski S. Analysis of tool wear in finish turning of titanium alloy Ti-6Al-4V under minimum quantity lubrication conditions observed with recurrence quantification analysis. Materials. 2025;18:79. https://doi.org/10.3390/ma18010079
41. Emami M, Karimipour A. Theoretical and experimental study of the chatter vibration in wet and MQL machining conditions in turning process. Precis Eng. 2021;72:41–58. https://doi.org/10.1016/j.precisioneng.2021.04.006
42. Zawada-Michałowska M. Thin wall milling at a maximized axial depth of cut. Materials. 2025;18:5219. https://doi.org/10.3390/ma18225219
43. Zawada-Michałowska M. Thin wall milling at a maximized axial depth of cut: an analysis of thermal and mechanical interactions. Materials. 2025;18:5347. https://doi.org/10.3390/ma18235347
44. Czyżycki J, Marciniak-Podsadna L, Twardowski P.

Classification of deflections of thin-walled elements made of EN AW-7075A aluminum alloy during milling. Adv Sci Technol Res J. 2023;17:301–14. https://doi.org/10.12913/22998624/174537

45. Xu Y, Yue C, Chen Z, Li M, Wang L, Liu X. Finite element simulation of residual stress in milling of aluminum alloy with different passes. Int J Adv Manuf Technol. 2023;127:4199–210. https://doi.org/10.1007/s00170-023-11795-2
46. Si-meng L, Xiao-dong S, Xiao-bo G, Dou W. Simulation of the deformation caused by the machining cutting force on thin-walled deep cavity parts. Int J Adv Manuf Technol. 2017;92:3503–17. https://doi.org/10.1007/s00170-017-0383-1
47. Agarwal A, Desai KA. Tool and workpiece deflection induced flatness errors in milling of thin-walled components. Procedia CIRP. 2020;93:1411–6. https://doi.org/10.1016/j.procir.2020.04.101
48. Li Z, Yan Q, Tang K. Multi-pass adaptive tool path generation for flank milling of thin-walled workpieces based on the deflection constraints. J Manuf Process. 2021;68:690–705. https://doi.org/10.1016/j.jmapro.2021.05.075
49. Gonzalo O, Seara JM, Guruceta E, Izpizua A, Esparta M, Zamakona I, et al. A method to minimize the workpiece deformation using a concept of intelligent fixture. Robot Comput Integr Manuf. 2017;48:209–18. https://doi.org/10.1016/j.rcim.2017.04.005
50. Weicheng G, Yong Z, Xiaohui J, Ning Y, Kun W, Xiao L. Improvement of stiffness during milling thin-walled workpiece based on mechanical/magnetorheological composite clamping. J Manuf Process. 2021;68:1047–59. https://doi.org/10.1016/j.jmapro.2021.06.039
51. Tehranizadeh F, Berenji KR, Saltuk Y, Budak E. Chatter stability of thin-walled part machining using special end mills. CIRP Ann - Manuf Technol. 2022;71:365–8. https://doi.org/10.1016/j.cirp.2022.04.057
52. Technical Data Sheet. https://www.tr-solution.pl/uploads/SILIKONY/Kondensacyjne/BLUESIL RTV 3318.pdf. Accessed 15 Jun 2026
53. International Organization for Standardization. ISO 37:2024 Standard - Rubber, vulcanized or thermoplastic. Determination of tensile stress-strain properties. 2024.
54. International Organization for Standardization. ISO 34-1:2024 - Rubber, vulcanized or thermoplastic. Determination of tear strength. Part 1: Trouser, angle and crescent test pieces. 2024.
55. SAE International. AMS4050K Standard - Aluminum Alloy, Plate 6.2Zn - 2.3Cu - 2.2Mg - 0.12Zr (7050-T7451) Solution Heat Treated, Stress Relieved, and Overaged. 2021.
56. Wang X, Song Q, Liu Z. Dynamic model and stability prediction of thin-walled component milling with multi-modes coupling effect. J Mater Process Technol. 2021;288:116869. https://doi.org/10.1016/j.jmatprotec.2020.116869
57. Navarro-Devia JH, Chen Y, Dao DV, Li H. Chatter detection in milling processes—a review on signal processing and condition classification. Int J Adv Manuf Technol. 2023;125:3943–80. https://doi.org/10.1007/s00170-023-10969-2
58. Damous M, Zeroudi N, Chellil A, Ikkache K. Prediction of a chatter stability of thin-walled parts during high-speed milling considering a variation of dynamic characteristics based on surface roughness measurement. Int J Adv Manuf Technol. 2023;127:5729–44. https://doi.org/10.1007/s00170-023-11945-6
59. Hashmi KH, Zakria G, Raza MB, Khalil S. Optimization of process parameters for high speed machining of Ti-6Al-4V using response surface methodology. Int J Adv Manuf Technol. 2016;85:1847–56. https://doi.org/10.1007/s00170-015-8057-3
60. Yiyang Z, Jian M, Gang L, Man Z. A review on error generation and control in efficient precision machining of thin-walled parts. Int J Adv Manuf Technol. 2024;133:2083–101. https://doi.org/10.1007/s00170-024-13813-3